Plant Soil (2020) 450:337–355
https://doi.org/10.1007/s11104-020-04446-y

REGULAR ARTICLE

A 3-dimensional model of *Pinus edulis* and *Juniperus monosperma* root distributions in New Mexico: implications for soil water dynamics

S. Schwinning · M. E. Litvak · W.T. Pockman · R.E. Pangle · A. M. Fox · C.-W. Huang · C.D. McIntire

Received: 12 August 2019 / Accepted: 2 February 2020 / Published online: 11 April 2020

Abstract
Aims (1) To develop a 3D root distribution model for piñon-juniper woodland using only tree species, sizes and locations as input. (2) To interpret a two-year time series of soil moisture relative to root distributions.
Methods The study was conducted in a piñon (*Pinus edulis* (Englem.)) -juniper (*Juniperus monosperma* (Englem.) Sarg.) woodland in New Mexico. We extracted roots from 720 soil blocks (30 cm × 10 cm × 10 cm) cut from the walls of three 10-m long and 1.5-m deep trenches. Roots were sorted by species and diameter class. Distribution models were developed for the dry weight of roots ≤5 mm in diameter. Soil water content and water potentials were measured in soil profiles under tree cluster and canopy gaps for 2 years, including a protracted dry-down period.
Results Piñon had twice the root dry mass of juniper, similar to the ratio of canopy projection areas. Root densities were ca. 50% lower in soils under canopy gaps compared to tree clusters and the species ratio did not significantly differ between clusters and gaps. Piñon root density declined faster with soil depth and distance from the stem compared to juniper. A hard caliche layer at 60–80 cm soil depth had no apparent effect on the already low root density at that depth. Overall, the models explained 66% (piñon) and 54% (juniper) of the spatial variation in root density at the scale of sampled soil blocks. During an 8-month dry period, soil moisture declined faster in regions of higher root density: in shallow soil and under tree clusters. This left a reserve of plant-available soil water in the deep soil under canopy gaps.
Conclusions Horizontal variation in root density in these open woodlands is predictable and an important component of the dynamic interactions between plant and soil. Under wet and dry conditions, soil water content is substantially different under tree clusters and canopy gaps.

Keywords Ecohydrologic heterogeneity · Patch connectivity · Root-model · Semi-arid woodland · Spatial heterogeneity · Spatial mosaic

Abbreviations
3D three-dimensional
ET Evapotranspiration

Introduction

Globally, plant roots return 40 - 60% of terrestrial precipitation as transpiration and thus play an important

Responsible Editor: Rafael S. Oliveira .

S. Schwinning (✉)
Department of Biology, Texas State University, 601 University Drive, San Marcos, TX 78666, USA
e-mail: schwinn@txstate.edu

M. Litvak · W. Pockman · R. Pangle · C.-W. Huang · C. McIntire
Department of Biology, University of New Mexico, MSC03 2020, Albuquerque, NM 87131, USA

A. Fox
School of Natural Resources and the Environment, University of Arizona, Tucson, AZ 85721, USA

role in the water cycle and climate feedbacks (Good et al. 2015; Schlesinger and Jasechko 2014). Roots also play a critical role in mediating the effects of climate and edaphic conditions on ecosystem function, including net primary production (NPP), hydrology and energy balance, especially in water-limited biomes (Warren et al. 2015). Information on 'rooting depth, distribution and dynamic uptake behavior' (Feddes et al. 2001) is therefore critical for parameterizing land surface models (LSMs), predicting vegetation-atmosphere interactions (Amenu and Kumar 2008; Bonan et al. 2014; Verhoef and Egea 2014) and community dynamics (Manoli et al. 2017). Yet, our understanding of feedbacks between root distribution and function remains cursory, particularly so for woody species with large root systems, where we are particularly dependent upon the synthesis of data from a variety of studies (e.g. Schenk and Jackson 2005).

The distribution of roots in the soil is part of plants' overall resource strategy, responsive to complex interactions between precipitation patterns, edaphic conditions and plant water uptake (Caylor et al. 2006). Understandably, roots reach their highest densities in the soil just below the surface, which is recharged most frequently by precipitation. Somewhat less predictably (Schenk 2008a), perennial plants also maintain deeper roots, in soil strata that are recharged less frequently, but whose residual water content may be able to sustain plants through a rainless period (Cubera and Moreno 2007; Ryel et al. 2010). Just how deep the root system of a species 'should' be is an unresolved question, although global trends of rooting depth with respect to climate, soil type and plant functional type have been documented (Fan et al. 2017; Schenk and Jackson 2002). However, even within communities and plant functional types, the root distributions of species differ in depth, spatial extent and density (Bucci et al. 2009; Fargione and Tilman 2005). Model predictions aside (Mirfenderesgi et al. 2019), there are few actual data that link species' resource strategies with root distributions. Moreover, an 'ideal' root strategy may not be realized if below-ground features such as hardpan or rock layers constrain root development (Renton and Poot 2014).

Here, we quantified the root distributions of piñon (*Pinus edulis* (Englem.)) and juniper (*Juniperus monosperma* (Englem.) Sarg.) in New Mexico, USA, two species already widely studied in terms of their differential drought responses (e.g. (Lajtha and Barnes 1991; Limousin et al. 2013; Meinzer et al. 2014; Morillas et al. 2017). Piñon-juniper woodlands are an extensive biome in North America (Pieper 2008) with well-documented responses to past and present climate change (Coats et al. 2008; Gray et al. 2006; Redmond et al. 2018) that can serve as a model system for understanding connections between root distribution, soil structure and plant function. Like other semi-arid woodlands worldwide, they are co-dominated by tree species with contrasting tolerance to to low water potenials (e.g., Aguade et al. 2015). They are typically patchy, a mosaic of tree clusters and canopy gaps aboveground (Martens et al. 1997; Ferreira et al. 2007) and a lesser known mosaic of rooting patterns belowground (Breshears et al. 1997). In such systems, it is particularly important to know both the vertical and lateral extent of tree roots by species to quantify patch connectivity and overall ecosystem function (Newman et al. 2010).

The overall goal of this study was to quantify the three-dimensional (3D) distribution of piñon and juniper roots in mixed woodlands, develop predictive models of root distributions for both species using aboveground tree locations and sizes as inputs and examine the relationship between spatial heterogeneity of root mass, rates of water extraction and the development of spatial gradients in soil water potential during drought. In particular, we sought to determine whether there are species differences in vertical and/or lateral root distribution and, as previously suggested (Breshears et al. 1997), juniper and piñon have differential access to soil under canopy gaps. We also explored whether soil calcification, at our site starting at 25 cm soil depth, influenced vertical root distributions.

Methods

Root collection

In March 2017, we excavated three trenches on a piñon-juniper dominated portion of a 6812 ha private ranch (Lat. 35.642, Long. -104.607, elevation 1925 m), ca. 56 km east of Las Vegas, New Mexico. The property had not been grazed by cattle since 2012. Mean annual precipitation in the region is 462 mm, the majority of which falls between May and October. Mean annual temperature is 10.5 °C (30 year means from PRISM Climate Group, Oregon State University, http://prism.oregonstate.edu, created 7 Dec 2019; Dataset: Norm81).

We laid out three 10 m trench lines that each started inside a tree cluster and ended in a gap between canopies. Live trees taller than 2 m within 10 m × 20 m rectangles

surrounding the trench lines were mapped by species and position relative to the trench line (Fig. 1). We recorded the height of trees, widest and perpendicular to widest canopy diameters and basal stem diameters (Table 1). The mapped trees were either *Pinus edulis* (Englem.) or *Juniperus monosperma* (Englem.) Sarg., with the one exception of a large *Juniperus scopulorum* tree near Trench 2. Unable to separate the roots of the two juniper species, we lumped this tree with all other juniper trees for analysis. There were no shrubs or cacti in the vicinity of the trenches and grass roots were easy to identify and were discarded. Soil structure was relatively consistent between trenches with a dark 15 - 35 cm thick organic topsoil turning into gravelly caliche, which turned into hard caliche at about 60–90 cm in Trenches 1 and 2, and 40–60 cm in Trench 3.

We cut the trenches on 20–21 March 2017 and completed root collections in one week. The day before excavation, trees within 1 m of the trench line were cut at ground level and removed to make space for the excavator. Trenches were dug with a 1 m wide bucket to 150 cm deep (the depth at which the excavator was rejected by bedrock).

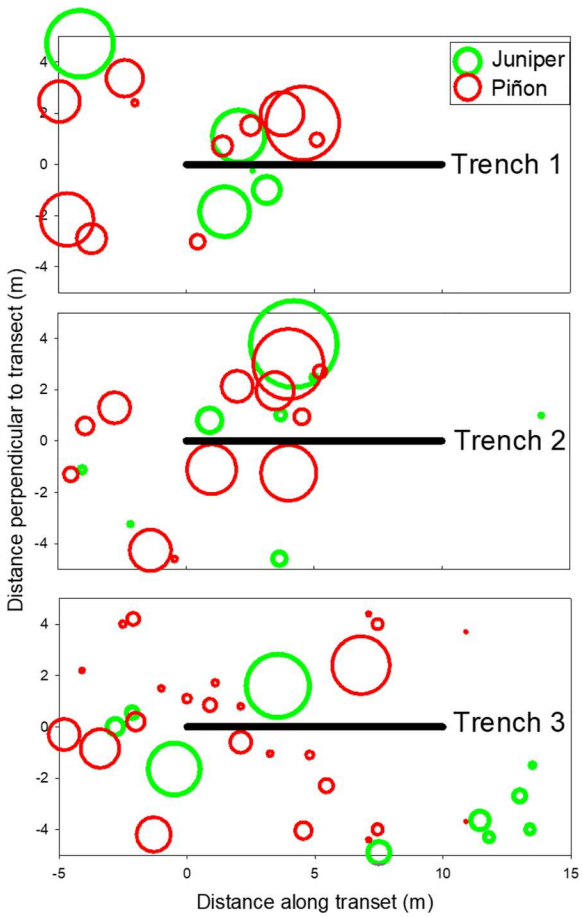

Fig. 1 Tree locations relative to transects 1–3. The three 10 m transects are indicted by the thick black lines. Bubble sizes approximate canopy projection areas. The bubble size shown in the legend corresponds to a canopy 1 m in diameter

In the trench, we sampled from the wall that was closer to the center of the tree cluster. We first smoothed the walls to a flat, vertical surface using hand tools, photographed them for future reference and cut roots protruding from the surface. We divided each trench into thirty 0.3 m segments and sampled every other segment, starting at 0.3 m on the trench line and ending at 9.6 m (e.g., 0.3–0.6 m, 0.9–1.2 m, …, 9.3–9.6 m: 16 segments). In each sampled segments, we cut soil blocks of 0.3 m width, 0.1 m height and 0.1 m depth out of the trench wall, put them on a tarp and broke then up by hand. Visible piñon and juniper roots were picked out and collected into plastic bags with a wet paper towel to maintain moisture. After this first pass, we sieved soils through a 2 mm wire mesh and retained roots were added to the first batch. We then inspected sieved soils for a final time to see if larger root fragments had been missed. We continued picking roots from the soil until 1 min. of searching did not result in any more roots being found. We assume that only short root fragments (e.g., < 3 cm) or thin primary roots (<< 0.8 mm) could have remained in the soil. This protocol was repeated for each segment to a depth of 150 cm. This sampling scheme yielded 240 individual sample blocks per trench; 16 in a row along the length of the trench and 15 per soil column between the surface and 150 cm depth. The root-filled plastic bags were locked air-tight and stored in chilled coolers on site until they could be refrigerated at the end of the day. Back at the labs we froze the root collections to avoid decomposition during months of analysis.

Root separation and measurement

We first separated roots by species based on color differences in bark and wood and the overall shape of roots. Juniper roots had a dark reddish-brown bark, were more fibrous with a high branching frequency and long roots had a more crooked appearance with frequent direction changes. In contrast, piñon long roots were lighter in color softer and more linear in growth (see also Pregitzer et al. 2002). We then separated roots from both species into four diameter size classes: > 20 mm, 5–20 mm, 0.8–5 mm and < 0.8 mm. Some root samples

Table 1 Composition of live trees (taller than 1 m) in 10 m × 20 m rectangular plots surrounding the trenches

	Piñon pine			Juniper		
	Tree number	Total canopy projection area (m2)	Total stem area (m^2)	Tree number	Total canopy projection area (m^2)	Total stem area (m^2)
Trench 1	12	115	0.237	10	62	0.171
Trench 2	13	130	0.198	8	49	0.067
Trench 3	31	102	0.228	11	71	0.109
Average	15.3	115.7	0.221	9.7	60.7	0.116

only consisted of fragmented fine roots ≤0.8 mm, which we did not attempt to separate by species. They were recorded as 'PJ' (mixed piñon and juniper).

We optically scanned roots ≤5 mm in diameter to determine root length and used the WinRhizo software package (Regent Instruments, Quebec, CA) to subclassify the roots into 12 diameter classes (0–0.8, 0.8–1.0, 1.0–1.5, 1.5–2.0. 2.0–2.5, 2.5–3.0, 3.0–3.5, 3.5–4.0, 4.0–4.5, 4.5–5.0, 5.0–6.0, 6.0–7.0, >7.0 mm). The fraction of >5 mm diameter roots should have been zero, but occasionally, the image analyzer detected significant root length in the >5 mm diameter classes. When this happened, the thick roots were picked out, reallocated to the corresponding 5–20 mm diameter batch and the remaining root sample rescanned. We followed the same protocol for roots <0.8 mm in diameter that were misplaced in a > 0.8 mm diameter batch. We dried all physically separated root batches at 70 °C and weighed them to get total root dry mass in each sample.

Root model development

Our goal was to develop a root model that quantifies spatial variation in water uptake capacity, a critical requirement for representing root function in land models. We know that the thinner (first order) roots, are most directly involved in water uptake (Freschet and Roumet 2017). Unfortunately, thinner roots are also harder to sample and separate by species (Addo-Danso et al. 2016). Therefore, the root fraction and metric chosen for model selection is a compromise between functional relevance and data quality.

Overall, 39% of the total measured root length was ≤0.8 mm in diameter and 86% was ≤2 mm in diameter (Table 2). Nearly half (45%) of the root length in these size classes could not be classified by species. Therefore, we decided to use the dry mass of roots ≤5 mm in diameter for modeling root distribution, instead of the root length density of fine roots. We assumed that the ≤5 mm dimeter class included both uptake roots and low branch-order transport roots, both of which are correlated with whole-plant water uptake capacity (Bouda et al. 2018). The *mass fraction* amounted to 29% of the total collected root dry mass and within it, only 8% of all root dry mass was unidentified by species. We divided the unknown root fraction equally among the two species for analysis.

Our overall approach to modeling root distributions was to identify, for each species, one function to characterize the attenuation of root density by soil depth and a second function to characterize the attenuation of root density with distance from individual trees. The product of the two functions predicts root density at any location in soil space. This framework makes the simplifying assumption that there is no interaction between vertical and horizontal root distributions, i.e., the shape of the vertical root distribution does not change with distance from a tree.

We did not sample the root mass of individual trees, only the root mass along three planar cuts through the soil. Therefore, we had to infer the contributions of individual trees to the total root biomass in a soil block, based on the number, the distance and the size of trees in the vicinity (Fig. 2).

To identify the best representation of vertical distribution, we fitted two models widely used in vegetation models; the exponential model (1) and the logistic dose-response model (2):

$$\overline{R_D} = \overline{R_0} * e^{-\delta D}, \tag{1}$$

$$\overline{R_D} = \frac{\overline{R_0}}{1 + \left(\frac{D}{D_{50}}\right)^C} \tag{2}$$

Table 2 Summary of root data from all three trenches by root diameter class and species. Data are reported as total root dry mass or length per ground area. This was calculated by summing all root quantities in the respective categories and dividing by 1.44 m^2, the total ground area sampled. Percent values in bold indicate the distribution of root quantity between species within a diameter class. Percent values in italic indicate the distribution of total root quantity between diameter classes

Root dry mass per ground area					
	< 0.8 mm dia. (kg m^{-2})	0.8 — 5 mm dia. (kg m^{-2})	5 — 20 mm dia. (kg m^{-2})	> 20 mm dia. (kg m^{-2})	All dia. classes (kg m^{-2})
Piñon	0.007 **(5%)**	0.813 **(69%)**	1.08 **(73%)**	1.16 **(65%)**	3.060 **(67%)**
Juniper	0.018 **(13%)**	0.362 **(31%)**	0.391 **(27%)**	0.624 (35%)	1.395 **(30%)**
Unidentified	0.120 **(82%)**	0.011 **(<1%)**	0	0	0.131 **(3%)**
Total	0.146 *(3%)*	1.186 *(26%)*	1.470 *(32%)*	1.782 *(39%)*	4.584 *(100%)*
Root length per ground area					
	< 0.8 mm dia. (m m^{-2})	0.8 — 2 mm dia. (m m^{-2})	2 — 5 mm (m m^{-2})	> 5 mm (m m^{-2})	All classes (m m^{-2})
Piñon	66 **(11%)**	345 **(47%)**	129 **(72%)**	5 **(21%)**	545 **(35%)**
Juniper	91 **(15%)**	240 **(33%)**	51 **(28%)**	19 **(79%)**	401 **(26%)**
Unidentified	449 **(74%)**	146 **(20%)**	0	0	598 **(39%)**
Total	604 *(39%)*	731 *(47%)*	180 *(12%)*	24 *(2%)*	1539 *(100%)*

in which $\overline{R_D}$ (kg m^{-2}) is cumulative average root mass per unit ground area from the bottom of the root zone to soil depth D and $\overline{R_0}$ (kg m^{-2}) is the cumulative average root mass per unit ground area from the bottom of the root zone to the soil surface. In the exponential model, δ is the exponential rate of root mass decline with soil depth. In the logistic model, D_{50} is the soil depth at the median of the root distribution (separating the upper and lower 50% of the root quantity) and C is a shape parameter. With one more parameter, the logistic model is more general than the exponential model and can, for example, fit unimodal root distributions, in which root density peaks below the soil surface.

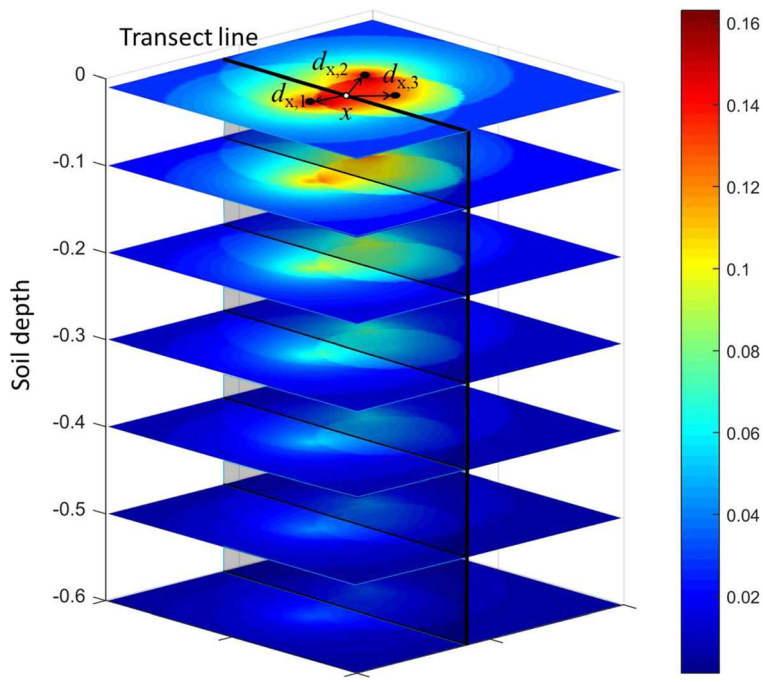

Fig. 2 Conceptual figure of modeling approach. The color scheme represents the variation of root density at different depths in the soil based on the locations of three trees (black circles). The black line marks the location of the transect. The three arrows indicate the horizontal distances of point x on the transect (white circle) to trees 1, 2 and 3. The model assumes that total root density at point x is the linear sum of contributions from trees 1,2 and 3

To derive a model for horizontal distribution, we took inspiration from the 'field-of-neighborhood' literature, which has developed a family of radially symmetric functions to model the attenuation of root activity by distance from the plant center (Berger et al. 2008). These models are usually scaled to the size of plants, so that a larger plant can have higher activity at equal distance from a point (i.e., trees with wider canopies can have wider root systems). In a preliminary analysis using vertically summed root dry mass for individually sampled segments on the transect, we determined that a simple exponential model with allometrically scaled canopy projection area produced the best fit with the least number of parameters:

$$\begin{aligned} R_{0,x} &= \omega + \textstyle\sum_{i=1}^{n_{x,\rho}} \left[fi * \varepsilon * A_i^{\alpha} * e^{-\beta d_{i,x}} \right] \\ (where)\ fi &= 1 \ if \ d_{i,x \le} \rho \\ fi &= 0 \ if \ d_{i,x} > \rho. \end{aligned} \tag{3}$$

Here, x is the midpoint of a transect segment, $R_{0,x}$ is the cumulative root mass per unit ground area from the bottom of the root zone to the soil surface at point x and $d_{i,x}$ is the distance between x and midpoint of the i'th tree in the vicinity (Fig. 1). The parameters ε and α are the allometric scaling parameters for the canopy projection area A_i of the i'th tree and β is a parameter that determines how fast root densities decline with distance from the tree. Parameter f_i ensures that only trees within a radius ρ from the sampling point (i.e., in the 'neighborhood of x') are included in the root tally.

Basically, the formula states that $R_{0,x}$ is determined by the sum of roots contributed individually by all trees in the neighborhood and that each contribution is weighted nonlinearly by the size and distance of the respective tree.

We found that the model fit was significantly improved by assuming a constant background root density ω, which does not occur in 'field-of-neighborhood' models, but in our model represented root mass that could not be attributed to any particular tree in the neighborhood.

The full spatial models (i.e., the product of functions 1 or 2 and 3) were

$$R_{D,x} = R_{0,x} * e^{-\delta D} \tag{4}$$

$$\text{and } R_{D,x} = \frac{R_{0,x}}{1 + \left(\frac{D}{D_{50}}\right)^{C}}. \tag{5}$$

with $R_{D,x}$ as the cumulative root mass per unit ground area from the bottom of the root zone to soil depth D at sampling point x on the transect. We determined the set of parameters (α, β, γ, δ (or D_{50} and C), ε, ω and ρ) that simultaneously minimized the sum of error squares between individual samples and point values predicted by the 3D model, using parameter values from the vertical and horizontal analyses as initial guesses. The parameter values slightly changed as the sum of error squares was minimized for all 720 individual samples, instead of for their vertical sums and horizontal averages.

For the goodness of fit analysis in Table 4 (the full model), prediction R^2 values were calculated using the following formula by (Alexander et al. 2015):

$$R^2 = 1 - \frac{\Sigma\left(y - \widehat{y}\right)^2}{\Sigma\left(y - \overline{y}\right)^2}, \tag{6}$$

where y is the observed root mass per ground area in blocks, $\widehat{y}$ is the predicted root mass per ground area calculated as $\left(R_{D_i,x} - R_{D_{i+1},x}\right)$ and $\overline{y}$ is the average observed root mass per ground area in blocks. The prediction R^2 values cited in Figure 4 (for horizontal distribution) uses the vertically summed root mass per ground area for y and $R_{0,\,x}$ for $\widehat{y}$.

Lastly, to determine how well the model predicted root distributions not used in model parameterization, we fitted models using the data from two trenches (every combination, in turn) to estimated root densities for the third, excluded trench. To distinguish between the two parameterization procedures, we refer to the '3-Trench Model' and the '2-Trench Model'.

Climate and soil data

The root excavation study was part of larger experiment involving nine 900 m^2 plots in this piñon-juniper woodland, including three plots in which all piñon tree were girdled, three plots in which all juniper trees were girdled and three control plots without girdling. We installed multiple sensors in these plots, which reported in 15 min intervals to data loggers. Here we are showing data only from the three control plots, as they are representative of the areas where root transect data were taken. Combined, the control plots contained 18 soil pits in which psychrometers (PST-55 psychrometer, Wescor ELITechGroup, Logan, UT) were inserted at 15, 30 and 60 cm depth and TDR probes (EC-5, Decagon Devices

Inc., Pullman, WA) at 5, 15, 30 and 60 cm depth. Of the six pits per plot, four were installed inside tree clusters and two in canopy gaps. Replicated soil water potential and water content data were reduced to daily averages across all replicated sensor positions. Daily changes in water content were calculated as the difference in the daily averages between consecutive days.

An on-site weather station (Campbell CR10X, Campbell Scientific, Logan, UT, USA) measured precipitation (TR-525USW, Texas Instruments, Dallas, TX) and air temperature (Campbell HMP45).

We also measured the predawn and midday plant water potentials of trees several times per year ($n = 5$ per species per plot) using pressure chambers (Model 1000, PMS Instrument Company, Albany, OR, USA). In the discussion, we refer to a measurement taken on 7 June, 2018.

Results

Root distribution

In the square plots surrounding the trenches (Fig. 1), the projected canopy area of piñon was roughly twice that of juniper (Table 1). Our root sampling from the trenches recovered 6.6 kg of root dry mass and 2.2 km of root length (Table 2). Across the three trenches, the average root mass of piñon was approximately twice that of juniper, roughly proportional to their canopy projection areas. At the maximal excavation depth of 1.5 m, 30% of the excavated soil blocks did not have any detectable root mass and those that did had only 0.18 g on average composed mostly of roots ≤0.8 mm in diameter that were lodged inside the narrow spaces of planar fractures. Thus, at 1.5 m, the rooting zone was very nearly at its outer limits.

The exponential model produced a slightly better fit it than the logistic model for both species (Table 3; Fig. 3). Model parameters indicate that piñon roots had overall shallower distribution with a median rooting depth of 25 cm compared to juniper's 31 cm. This difference was highly significant (t-test: $p < 0.0001$), however, the difference in the shape parameter C was not (t-test: $p = 0.58$). The average root density of piñon exceeded that of juniper down to a depth of 80 cm, below, juniper roots were more abundant than piñon roots.

The parameterization of the full 3D produced a nearly equally good fit regardless of which model was used to model root attenuation with soil depth (Table 4). Parsimony would therefore favor the exponential model. Besides the species difference in vertical root distribution, the other main difference was in species' effective neighborhood radius (ρ, Table 4): In piñon, root densities were elevated above background levels only within 2 m of a tree bole, whereas that radius was 4 m for juniper. At the same time, the background density of root mass (ω) was ca. twice as high for piñon than for juniper.

The prediction of horizontal root distribution based on the numbers, locations and sizes of trees in the neighborhood of sampling points (Fig. 4) was considerably less accurate than for vertical distribution (Fig. 3). Nevertheless, the model correctly captured the general decline of root densities between clusters and adjacent canopy gaps. Moreover, predictions of the 2-Trench Models (which were parameterized only with data from the two trenches not predicted) were quite similar to the 3-Trench Model, suggesting that the parameterized model can potentially be applied to sites with similar tree density and soil condition.

Along the trenches, the vertically summed root densities of piñon exceeded those of juniper by about 2:1 (Fig. 5: note the change in color scale, Fig. 7). The models captured the tendency for roots under tree clusters to be both denser and deeper than under canopy gaps. Roots were most concentrated above the caliche. In the friable caliche between ca. 30 and 80 cm, root densities where quite patchy. Species differences in rooting depth were particularly obvious in Trench 1, which had the highest local concentration of large juniper trees (Fig. 1). Below 80 cm, inside the hard caliche, roots of both species were sparse and patchily distributed. This was particularly observable in Trench 2, in which the caliche below 80 cm was very strongly cemented and minimally fractured.

Soil moisture dynamics

During the first two years of data collection, there was a prolonged dry period from November 2017 through June 2018 (Fig 6a). Soil water potentials dropped precipitously during this interval across soil depths (Figs 6b-d). Because the soil psychrometers used to measure soil water potential are less sensitive under near-saturating conditions, water potentials tend to flatline during wet intervals. During drought, these sensors

Table 3 Results of the vertical root distribution analyses using the spatial averages across all three trenches. The prediction R^2 is the R^2 of the regression between predicted (x) and measured (y) root density for individual layers. $\overline{R_0}$ is the average vertically summed root dry mass from the bottom to the root zone to the soil surface

	Piñon root dry mass (≤5 mm dia.)	Juniper root dry mass (≤5. 5 mm dia.)
Exponential model		
$\overline{R_0}$ (kg m^{-2})	1.08 (0.01)	0.52 (0.008)
a	0.036 (0.0007)	0.026 (0.006)
Prediction R^2	0.966	0.934
Logistic dose-response model		
$\overline{R_0}$ (kg m^{-2})	0.90 (0.02)	0.46 (0.008)
D_{50} (cm)	25 (0.08)	31 (0.8)
C	2.2 (0.1)	2.0 (0.06)
Prediction R^2	0.921	0.881

are superior to other probes in quantifying meaningful limits on plant-available water (Jones 2007).

Soil water potentials became limiting to plant water uptake at different times, depending on soil depth and location (i.e. cluster vs. gap). For the purpose of discussion, we use −1 MPa as a reference state. For example, soil water potentials under tree clusters fell below −1 MPa first at 15 cm depth, ca. 6 weeks later at 30 cm depth and an additional 5 weeks later at 60 cm depth. Soil in gaps passed the same −1 MPa mark

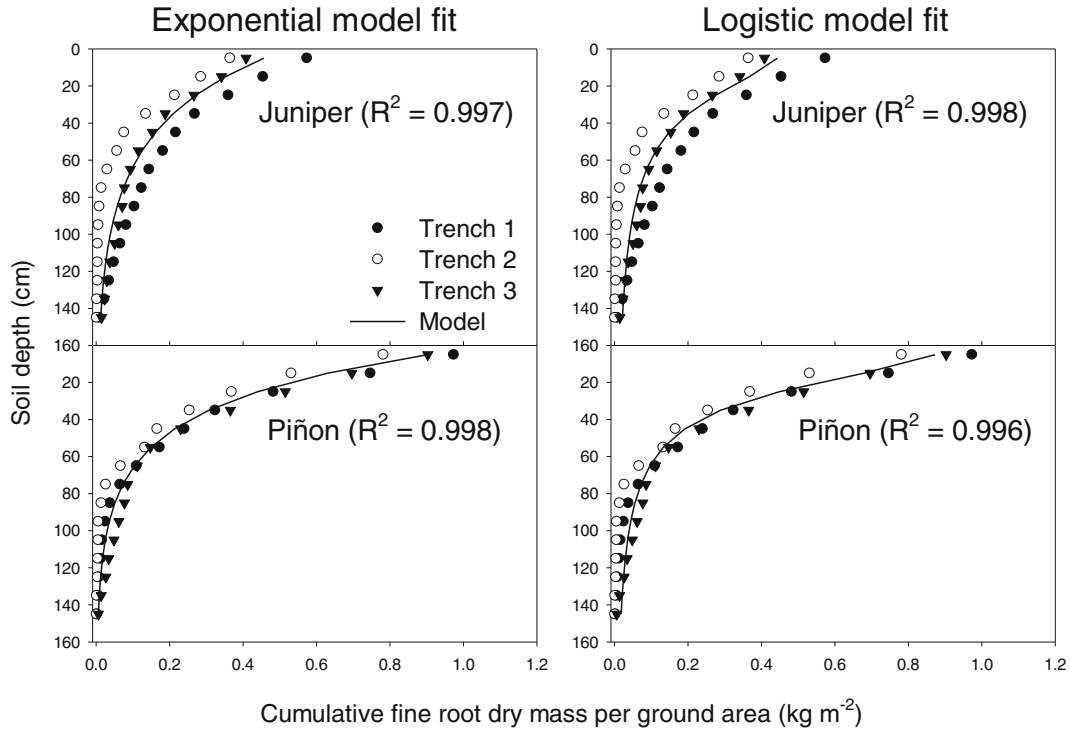

Fig. 3 Model solutions and data for horizontally averaged dry mass of roots ≤5 mm diameter. Data were collected in 10 cm increments from the surface to 150 cm depth. On the left, root dry mass per ground area was fitted to the exponential model; on the right to the logistic dose-response model. The R^2 values are the adjusted R^2 values of the regression. Corresponding model parameters are shown in Table 3

Table 4 Variable and parameter names, meaning and values of the 3D root models for piñon and juniper

A. Variable ranges		Values piñon	Values juniper
D	Soil depth	5–145 cm	5–145 cm
$d_{i,x}$	Distance of the i'th tree from poim x on the transect	Up to 2 m	Up to 4 m
n_x	Number of trees within a within a radius of ρ m around point x	0–4	0–4
A_i	Canopy projection area of i'th tree in the neighborhood	0.7–22.8 m^2	0.52–26.9 m^2
B. Exponential model			
ε	Linear allometrict scaling factor	0.31	0.096
α	Allometric scaling power	0.23	0.72
β	Constant of exponential decay of root density with distance from tree	0.41	0.65
ρ	Neighborhood radius	2 m	4 m
ω	Background root mass per ground area	0.62 kg m^{-2}	0.30 kg m^{-2}
δ	Constant of exponential decay of root density with soil depth	0.035	0.025
Prediction R^2	R^2 of the regression between prediction (x) and observation (y) at the level of individual samples	0.66	0.54
C. Logistic dose-response model		Values piñon	Values juniper
ε	Linear allometric scaling factor	0.248	0.082
α	Allometric scaling power	0.23	0.73
β	Constant of exponential decay of root density with distance from tree	0.38	0.64
ρ	Neighborhood radius	2 m	4 m
ω	Background root mass per ground area	0.52 kg m^{-2}	0.26 kg m^{-2}
D_{50}	Depth of median root distribution	26 cm	32 cm
C	Shape parameter for vertical root distribution	2.2	1.9
Prediction R^2	R^2 of the regression between prediction (x) and observation (y) at the level of individual samples	0.64	0.53

additional weeks later at each depth. In the densest region of the root zone (15 cm under cluster), the soil dried to −1 MPa by January 2018 (Fig. 6b), while in peripheral regions (60 cm under gap), the soil had dried to the same level by May 2018 (Fig. 6d).

The soil water potentials between cluster and gap initially diverged under drought (Figs 6b-d), as soil water was lost more quickly from clusters than from inter-canopy gaps (Figs 6e-g). Since soil water loss also declined with soil depth, water potentials diverged faster at 15 cm than at 30 cm depth and most slowly at 60 cm depth. Over time, despite the difference in root density, water uptake rates between clusters and gaps tended to equalize, almost immediately at 15 cm depth (Fig. 6e) and several months into the drought at 60 cm depth (Fig. 6g). When compared at equal water potentials during the dry-down period, water loss was faster from clusters than gaps, but only in the range from 0 to −1 MPa soil water potential (Fig. 8).

Differences were also observable during periods of recharge (Fig. 6b-d: 5/17–10/17 and 7/18–11/18). Particularly at 60 cm depth, soil under canopy gaps was initially drier than in tree clusters. However, over the course of several months, soil moisture under both clusters and gaps equalized.

Discussion

Modeling root distributions in three dimensions

It is clear in the literature that root distributions in forests and woodlands are spatially variable, especially so in semi-arid woodlands, which are often structured into distinct tree clusters, separated by open areas (gaps in the canopy) of bare soil and herbaceous cover (Breshears 2006). Heterogeneity of land cover is an important modifier of ecosystem function (Newman et al. 2010), but while land models have become more sophisticated in representing the heterogeneous distribution of canopies, they have failed to do so for the rhizosphere (reviewed in Fisher et al. 2018).

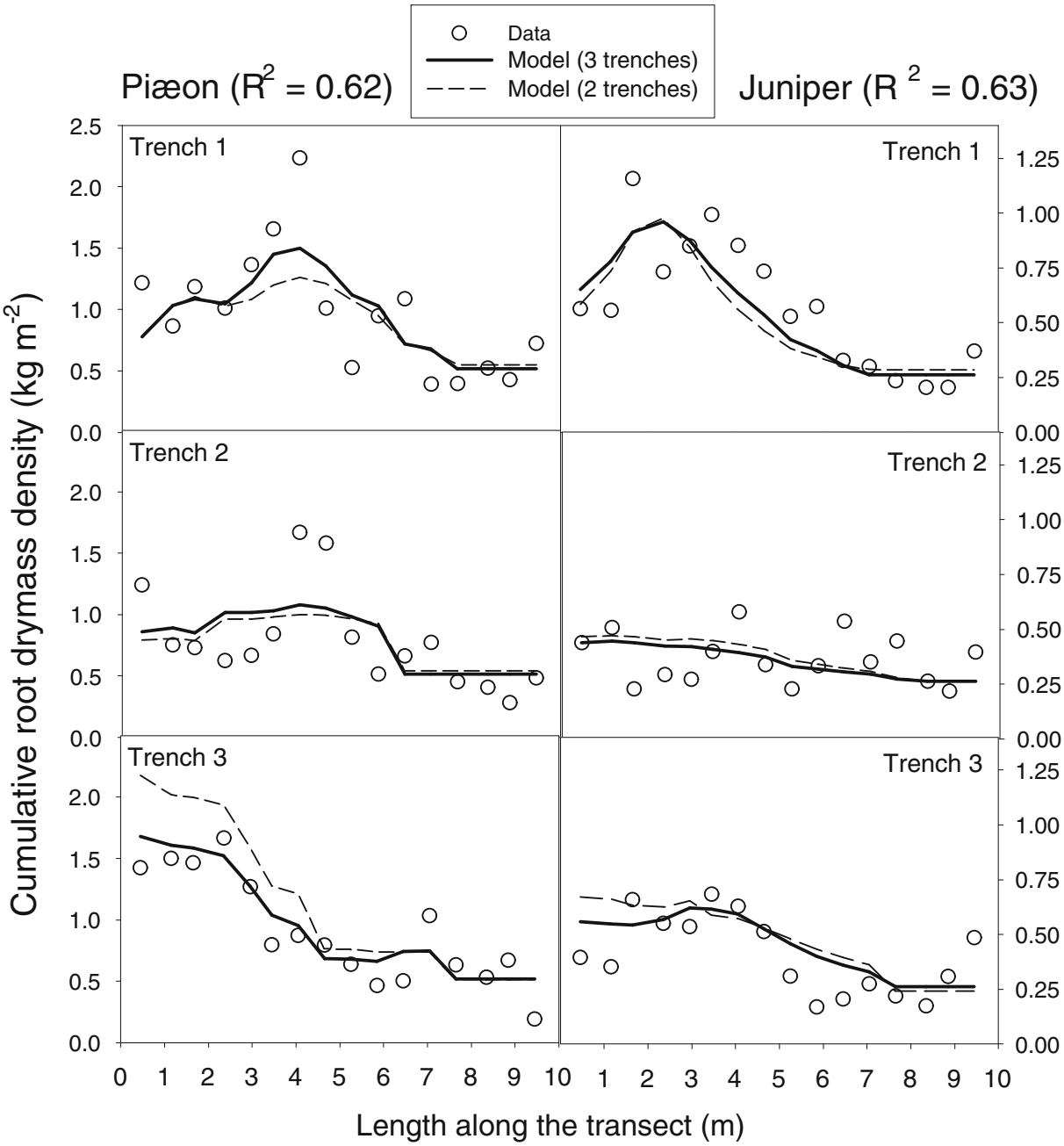

Fig. 4 Model solutions and data for vertically summed, horizontal fine root distribution (*Rx,0*) along points x on the respective transects. The 3-Trench model was parameterized using all three trenches. The 2-trench model was parameterized with two trenches excluding the trench for which root densities were estimated. Each transect started inside tree clusters (at 0 m) and ended inside canopy gaps (at 10 m). The R^2 values correspond to the goodness of fit of the 3-Trench model across all trenches. The model was the exponential version (Table 4). Note the difference in scale between the left- and right-hand figures

We demonstrate that above-ground patterns of tree distribution in a semi-arid open woodland can be used to predict at least coarse patterns of root distribution below-ground, such as differences in root densities between tree clusters and canopy gaps (Fig. 4). This was achieved by fitting a relatively simple 6-parameter model, which assumed no interaction between vertical and horizontal root distribution nor between the root

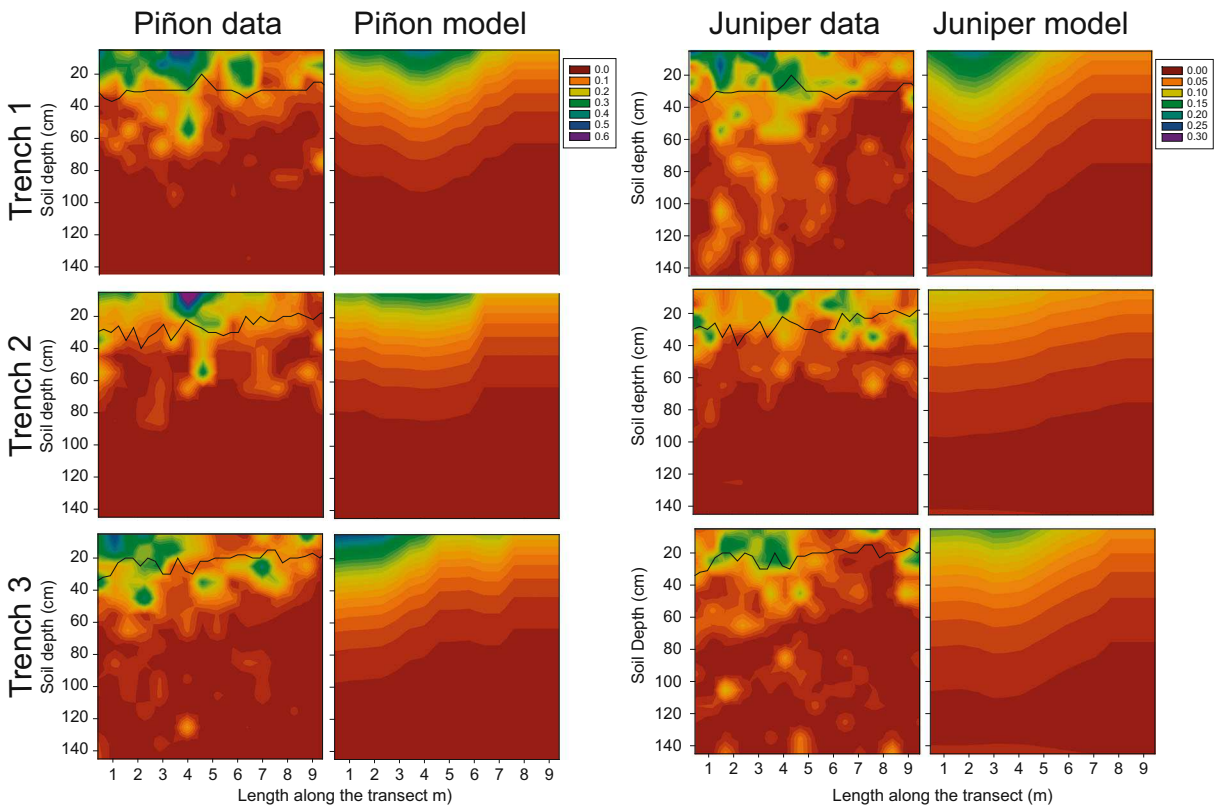

Fig. 5 Kriged maps of model solutions and data for the three trench walls. Colors are scaled linearly to the dry mass density per ground area in 10 cm layers (kg m^{-2}) of roots ≤5 mm in diameter. The lines indicate the observed depth of the transition between dark organic soil to white, friable caliche. Note the difference in scale between piñon and juniper. Each transect started inside tree clusters (at 0 m) and ended inside canopy interspaces (at 10 m). Corresponding model parameters are shown in Table 4

systems of individual trees (e.g., contact avoidance; Brisson and Reynolds 1994). This simple structure is an important feature, since it suggests that easier sampling protocols could be used to parameterize 3D root models in future studies. For example, it should be sufficient to sample only the topsoil layer (containing 30–50% of all roots) and then couple the horizontal distribution term to a known or independently determined vertical root distribution term.

The model captured approximately 60% of the variation in the horizontal cumulative root density ($R_{0,\,x}$) at the scale of 300 cm^2 patches of ground area (unexplained variation in vertical space was diminishingly small by comparison). The model was fairly successful predicting variation in the root density gradient between clusters and gaps (e.g., for example the difference between the shallow gradient for juniper in Trenches 2 & 3 and the steep gradient for piñon in Trenches 1 & 3; Fig. 4). Part of the unexplained variation was contributed by patches of unusually high root density. The model also failed to link local root densities to tree locations at greater distances, which made it necessary to incorporate the 'background' root density parameter (ω), a minimal value for root density in gaps. It should be assumed that this value in particular will change with the average size of canopy gaps.

According to Schenk and Jackson (2002), more than 90% of all root profiles globally have at least 50% of their roots in the top 30 cm. The root profile of this piñon-juniper woodland was no different: More than half of the dry mass of roots ≤5 mm were in the organic soil layer, which had a variable depth between 15 and 35 cm (24 cm on average; Fig. 5). Below, a layer of friable caliche was also well-populated by roots of both species. There was no apparent discontinuity in vertical root distribution to suggest that the calcified soil layers

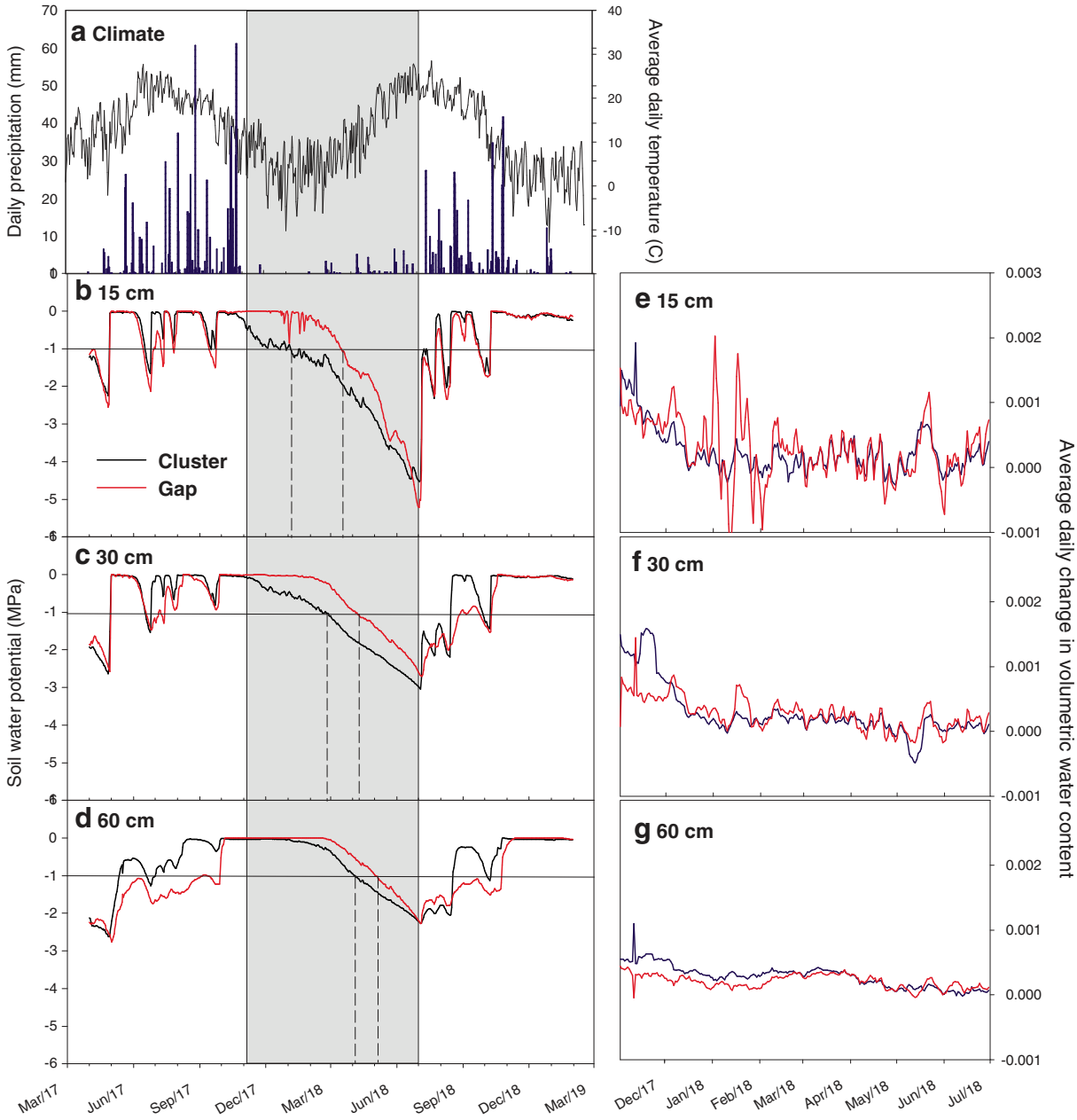

Fig. 6 Climate and soil moisture over two years. **a**: Daily precipitation and average temperature; **b-d**: soil water potentials at 15 cm, 30 cm and 60 cm depth from 1 April 12,017 to 31 January 2019. The highlighted window marks 8 months of low precipitation in which the soil dried out. The vertical dashed lines highlight the dates when soil water potentials fell below – 1 MPa. **e-g**: Daily changes in soil water content over this 8-month period are shown in the right column (**e-g**) as 10-day running averages. Positive values indicate soil water loss, negative values soil water gain. In Figures **b-g** dark-blue lines represent soil sensors under tree clusters and red lines soil sensors under canopy gaps

imposed a significant barrier for vertical root growth (Fig. 3). A hard caliche layer came in at ca. 80 cm depth that was more likely to present a barrier for root growth. However, at that depth root densities were already quite low (Fig. 1). Therefore, we conclude that patterns of soil calcification at our study site had minimal effects on root distributions or in constraining plant water access under most conditions.

Species differences

Our study provides the first direct evidence of differences in root distribution between piñon and juniper. Early investigators speculated, based on ecophysiological observations, that juniper may be shallower-rooted than piñon (Lajtha and Barnes 1991). But a recent study using stable isotope tracers concluded that juniper used deeper water sources than piñon during drought, likely including water taken up from fractured bedrock below 50 cm soil depth (Grossiord et al. 2019). In our study, juniper trees also had deeper roots, but species differences were moderate.

Relative root mass (for roots ≤5 mm diameter) in the top 20 cm of the soil was 1.3 x greater for piñon than for juniper and piñon had a median rooting depth (D_{50}) of 26 cm compared to juniper's 32 cm (Table 4). The portion of total root mass that was present below 80 cm in the fractured rock represented 5% for piñon compared to 13% for juniper.

Previous studies suggested that juniper has a spatially more expansive root structure than piñon (Breshears et al. 1997). In Breshears et al. (1997), when water was applied to open spaces surrounding isolated trees, juniper was physiologically more responsive than piñon and water disappeared faster adjacent to juniper. By contrast, we could draw no clear distinction between piñon and juniper lateral rooting width in this study. While piñon trees did form patches of very high root density close to their stem, they also maintained root mass in gaps (Figs. 4 and 5). Juniper trees generally did not concentrate roots near the stem as much and showed a more gradual decline of density between cluster and gap (Fig. 4). Neither species appeared to have the advantage accessing soil under gaps and the species ratio of root mass was similar between cluster and gap (Appendix Fig. 7).

In the models, the difference in lateral distribution was reflected most clearly in the neighborhood radius (parameter ρ, Table 4), the maximal distance from the tree center at which root densities were elevated above background levels. According to the regression results, that radius was 2 m for piñon roots versus 4 m for juniper. However, piñon also had a higher background root density than juniper (parameter ω). These patterns could be consistent with a more adaptive (therefore less predictable) root distribution in piñon.

We based our spatial analysis on the dry mass of roots ≤5 mm in diameter, 29% of the total root dry mass (Table 1) and deliberately excluding thick structural roots. The decision to analyze root dry mass rather than root length was driven in part by the low accuracy for identifying fine roots by species. This biased the analysis towards thicker roots in the 0–5 mm diameter range, a set that was likely dominated by low branch-order transport roots. Although recent models suggest that axial conductance of transport roots can co-limit network conductance (Bouda et al. 2018), we cannot expect the distribution of transport roots to match that of absorptive roots exactly. If roots have regular branching patters, we may assume that the length and mass of roots with higher branching order has an approximately allometric power-relationship with the length of roots with lower branching order, all the way down to the primary absorbing roots (Arrendondo and Johnson 2011). Thus, if root mass M declines exponentially with soil depth or distance from a tree d ($M_d \sim e^{-\alpha d}$) and the length of absorbing roots L has an allometric relationship to the mass of higher order transport roots to which they attach ($L_d = \beta M_d^{\gamma}$), it follows that the distribution of absorptive root length would have a different exponential distribution parameter ($L_d \sim \beta e^{-\alpha\gamma d}$). Different species may very well have different allometries and in addition, allometric relationship may change with soil depth and season (Peek et al. 2006). Thus, species differences in parameters of root mass distribution should be interpreted with caution. Differences in terminal branching patterns could accentuate or diminish differences in the spatial distribution of resource uptake capacity.

Woody plant species in water limited environments often have expansive root systems with both deep tap roots and long lateral roots; the evergreen shrub *Larrea tridentata* is a good example (Brisson and Reynolds 1994; Gile et al. 1998; Schwinning and Hooten 2009). These species are adapted to extracting soil water year-round, which includes times when soil water potentials are low and contain only a small fraction of plant-available water by volume. Such species increase their water uptake more effectively by accessing a greater soil volume rather than by increasing root density (Hartle et al. 2006). Species with lower tolerance for low water potentials are by contrast adapted to optimizing water uptake during times of relatively high soil water availability. Exemplified by *Ambrosia dumosa,* these species have higher fine root density with a higher proportion of shallow roots (Hartle et al. 2006; Schwinning and Hooten 2009). Part of their strategy may also include a more adaptive spatial root allocation, which increases in pockets of high soil moisture (Wilcox et al. 2004). We suggest that the contrasting ecophysiology and

root distributions of *L. tridentata* and *A. dumosa* of the Mojave Desert, similar to piñon and juniper, exemplify a general pattern of species differentiation between co-dominant woody plants in water-limited environments.

Soil water dynamics

Spatial heterogeneity of soil moisture is a key aspect of the ecohydrology of water-limited systems (Breshears and Barnes 1999), enabling such critical functions as niche separation and coexistence (Walter and Mueller-Dombois 1971), drought persistence (Ryel et al. 2010) and hydraulic redistribution (Neumann and Cardon 2012). These phenomena have been investigated primarily with a focus on vertical heterogeneity but horizontal variability could be as important. We focused here on differences between tree clusters and canopy gaps, being the more predictable component of spatial variability (Fig. 4). However, we note that a finer grain of spatial variability, related to the clustering of roots in soil pockets (Fig. 5), probably adds another significant component of heterogeneity.

Most of the time, soil water potentials were different in clusters and gaps at equal depth (Fig. 6), but the gradient inverted in periods of recharge vs. dry-down. Recharge in gaps lagged behind clusters, which left gaps drier during much of the recharge periods. This may be caused by precipitation redistribution from canopy gaps to tree clusters by overland flow (Reid et al. 1999). Ponding may occur in gaps where the absence of stem flow and vertical macropores along root channels (Luo et al. 2019) slow infiltration.

Conversely, during an extended period in which the soil dried out, soil under canopy gaps maintained less negative water potentials for longer than soil under tree clusters. At every soil depth, rates of water loss were initially higher in tree clusters (Fig. 5 e-g), as would be expected with roughly twice the root density. Interestingly, rates of water loss between cluster and gaps converged over time, suggesting that the lower root hydraulic conductance in soil under canopy gaps (which would have slowed water uptake) was increasingly compensated by a steeper soil-to-root water potential gradient (which would have increased water uptake). When compared at the same soil water potential, water loss from regions of higher root density under cluster was predictably higher than under canopy gaps, at least at water potentials above -1 MPa (Appendix Fig. 8). At more negative soil water potentials, differences in water loss rates between cluster and gap were no longer evident, perhaps because they were too low to be detectable or because other processes than root water uptake dominated (diffusion, redistribution).

In Fig. 6, we highlighted the sequence in which soil water potentials passed through −1 MPa to illustrate that some regions of the soil maintained a relatively high level of plant-available water for months into the drought. However, the volume of these relatively wet soil regions progressively contracted, at last restricted to deep soils (≥ 60 cm) under canopy gaps. For piñon, which can take up water only from soils with less negative water potentials, that contraction would have happened at a faster pace than for juniper.

For example, on 7 June 2018, average midday water potentials was −1.8 MPa for piñon, which would have allowed trees to extract water just barely from gaps at 60 cm soil depth, where soil water potential was still at −1.6 MPa. By that time, piñon had probably severed hydraulic connections to most of the soil volume above 60 cm depth and might have been close to ceasing water uptake (and transpiration) entirely. At the same time, the average midday water potential of juniper was −2.7 MPa, suggesting that juniper still extracted water from gaps at 30 cm soil depth (cluster: −2.6 MP; gap: −2.0 MPa), and both cluster and gap at 60 cm depth (cluster: −1.9 MPa and gap: −1.6 MPa).

For both species, but especially piñon, soil moisture retained in gap locations should have helped trees avoid damaging levels of desiccation, but low rooting density would have also restricted daytime transpiration. Thus, what Ryel et al. (2010) called the plant 'maintenance pool' of soil moisture may be interpreted as a byproduct of spatial heterogeneity in root distribution and should be located at the periphery of root systems. Both the exponential decline of root density with depth (Fig. 3) and with distance from the root crown (Fig. 4) may be caused by constraints of root development. But it is intriguing to consider that natural selection can fine-tune plant rooting patterns, not just to optimize overall water and nutrient uptake while minimizing costs (Schenk 2008b), but also to moderate fluctuations in plant water status. Thus, relatively small variation in root allocation to the 'maintenance pool' could influence survival during prolonged periods of drought.

Persistent soil water potential differences between tree cluster and canopy gap locations also suggest the possibility of lateral hydraulic redistribution. Juniper

might be better suited to this function, due to potentially longer lateral roots and greater water-potential bandwidth for hydraulic transport (Sperry et al. 2016). Hydraulic redistribution should occur in the direction of gaps during periods of soil water recharge following observed water potential gradients, and in the direction of tree clusters during drought. However, as observed in other studies, the amounts of water transported in this way would not be large, since after all, substantial gradients in soil water potentials were maintained.

Summary

We conducted an extensive root excavation study in a piñon-juniper woodland in New Mexico to develop a 3D root distribution model that used as input the distances and sizes of trees in the neighborhoods of sampling points. We found that it was possible to link heterogeneity in canopy cover to heterogeneity of root densities below ground, using two negative exponential functions to characterize the attenuation of root density with vertical distance from the soil surface and with horizontal distances from plant stems. The simplicity of the model suggests that it may apply to other patchy woodlands.

The two species had similar maximal rooting depths, but piñon, which is less tolerant to negative soil water potentials, had a greater concentration of finer root mass (≤5 mm root diameter) in shallow soil layers and close to tree trunks compared to juniper. Average root mass densities for both species was approximately half under canopy gaps than under tree clusters. Soil water depletion under gaps was delayed during drought, which preserved plant-available water under canopy gaps for both species.

Current ecosystem-scale modes represent root systems as either perfectly mixed or perfectly separated between vegetation cover types. Either assumption is unrealistic and would fail to predict the actual length of time for which plant-available water remains in the soil during drought. Modeling intermediate horizontal connectivity below ground would require novel transfer functions for carbon (roots), nutrients and water between vegetation subclasses.

Appendix

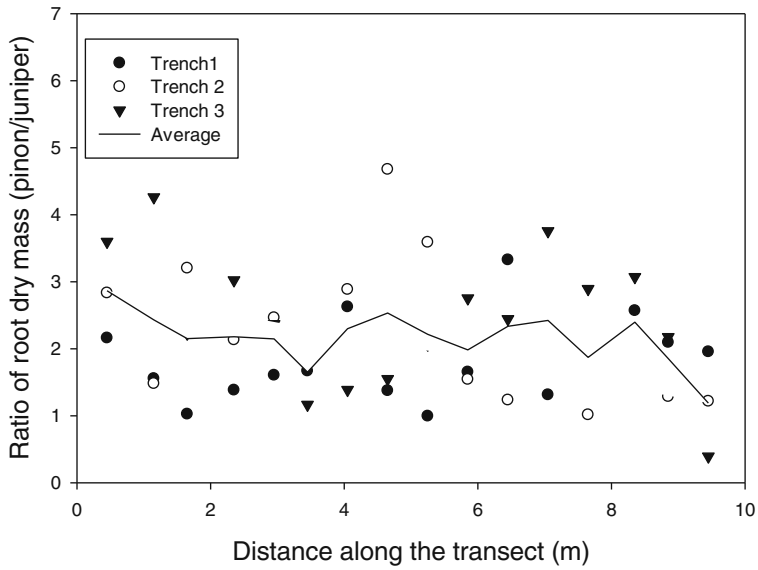

Fig. 7 Ratio of vertically summed piñon and juniper root dry mass in the ≤5 mm diameter class

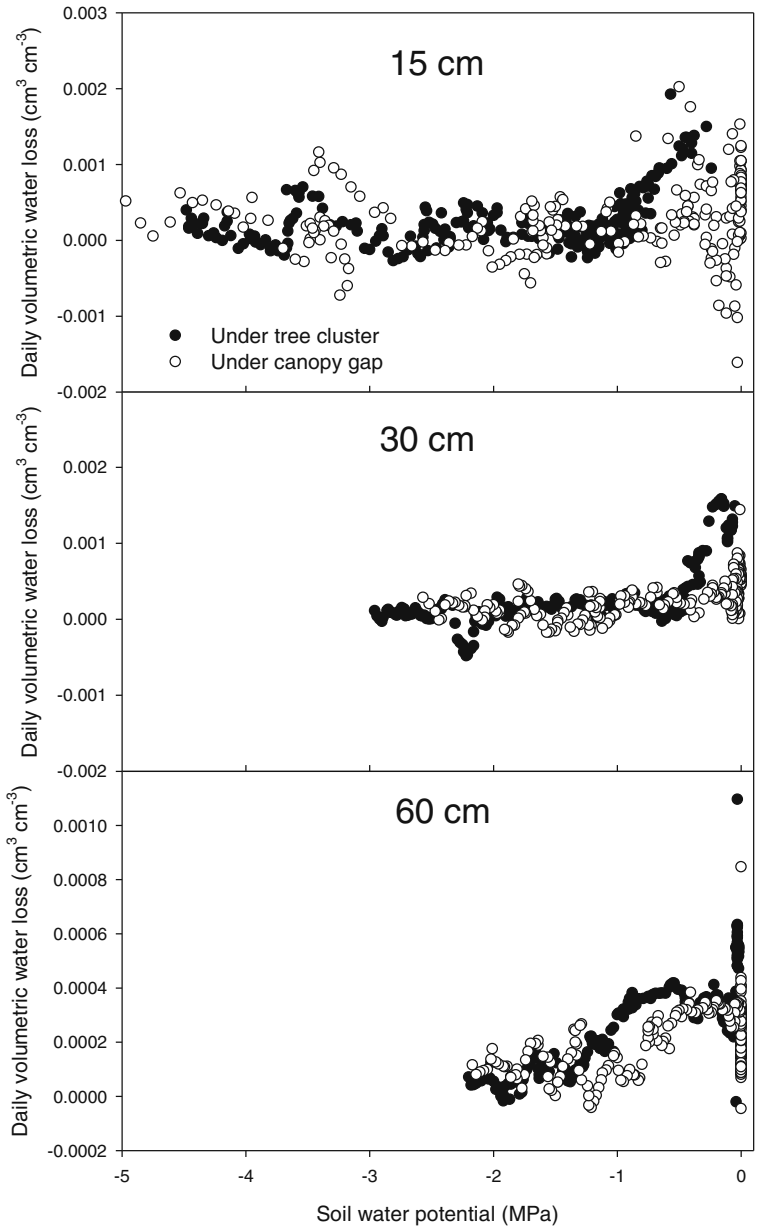

Fig. 8 Daily change in soil water volumetric content (positive values = loss) against soil water potential. Data are shown for the period between 1 November 2017 and 30 June 2018. At equal water potentials in range of 0 and − 1 MPa, water loss from tree clusters (where root density is higher) exceeds water loss from canopy gaps

References

Addo-Danso SD, Prescott CE, Smith AR (2016) Methods for estimating root biomass and production in forest and woodland ecosystem carbon studies: a review. For Ecol Manag 359:332–351. https://doi.org/10.1016/j.foreco.2015.08.015

Aguade D, Poyatos R, Rosas T, Martinez-Vilalta J (2015) Comparative drought responses of Quercus ilex L. and Pinus sylvestris L. in a montane Forest undergoing a vegetation shift. Forests 6:2505–2529. https://doi.org/10.3390/f6082505

Alexander DLJ, Tropsha A, Winkler DA (2015) Beware of R-2: simple, unambiguous assessment of the prediction accuracy of QSAR and QSPR models. J Chem Inf Model 55:1316–1322. https://doi.org/10.1021/acs.jcim.5b00206

Amenu GG, Kumar P (2008) A model for hydraulic redistribution incorporating coupled soil-root moisture transport. Hydrol Earth Syst Sci 12:55–74. https://doi.org/10.5194/hess-12-55-2008

Arrendondo JT, Johnson DA (2011) Allometry of root branching and its relationship to root morphological and functional traits in three range grasses. Journal of Experimental Botany 62: 5581–5594. https://doi.org/10.1093/jxb/err240

Berger U, Piou C, Schiffers K, Grimm V (2008) Competition among plants: concepts, individual-based modelling approaches, and a proposal for a future research strategy. Perspect Plant Ecol Evol Syst 9:121–135. https://doi.org/10.1016/j.ppees.2007.11.002

Bonan GB, Williams M, Fisher RA, Oleson KW (2014) Modeling stomatal conductance in the earth system: linking leaf water-use efficiency and water transport along the soil-plant-atmosphere continuum. Geosci Model Dev 7:2193–2222. https://doi.org/10.5194/gmd-7-2193-2014

Bouda M, Brodersen C, Saiers J (2018) Whole root system water conductance responds to both axial and radial traits and network topology over natural range of trait variation. J Theor Biol 456:49–61. https://doi.org/10.1016/j.jtbi.2018.07.033

Breshears DD (2006) The grassland-forest continuum: trends in ecosystem properties for woody plant mosaics? Front Ecol Environ 4:96–104. https://doi.org/10.1890/1540-9295(2006)004[0096:tgctie]2.0.co;2

Breshears DD, Barnes FJ (1999) Interrelationships between plant functional types and soil moisture heterogeneity for semiarid landscapes within the grassland/forest continuum: a unified conceptual model. Landsc Ecol 14:465–478. https://doi.org/10.1023/a:1008040327508

Breshears DD, Myers OB, Johnson SR, Meyer CW, Martens SN (1997) Differential use of spatially heterogeneous soil moisture by two semiarid woody species: Pinus edulis and Juniperus monosperma. J Ecol 85:289–299. https://doi.org/10.2307/2960502

Brisson J, Reynolds JF (1994) The effect of neighbors on root distribution in a CREOSOTEBUSH (LARREA-TRIDENTATA) population. Ecology 75:1693–1702. https://doi.org/10.2307/1939629

Bucci SJ, Scholz FG, Goldstein G, Meinzer FC, Arce ME (2009) Soil water availability and rooting depth as determinants of hydraulic architecture of Patagonian woody species. Oecologia 160:631–641. https://doi.org/10.1007/s00442-009-1331-z

Caylor KK, D'Odorico P, Rodriguez-Iturbe I (2006) On the ecohydrology of structurally heterogeneous semiarid landscapes. Water Resour Res 42. https://doi.org/10.1029/2005wr004683

Coats LL, Cole KL, Mead JI (2008) 50,000 years of vegetation and climate history on the Colorado plateau, Utah and Arizona, USA. Quat Res 70:322–338. https://doi.org/10.1016/j.yqres.2008.04.006

Cubera E, Moreno G (2007) Effect of single Quercus ilex trees upon spatial and seasonal changes in soil water content in dehesas of central western Spain. Ann For Sci 64:355–364. https://doi.org/10.1051/forest:2007012

Fan Y, Miguez-Macho G, Jobbagy EG, Jackson RB, Otero-Casal C (2017) Hydrologic regulation of plant rooting depth. Proc Natl Acad Sci U S A 114:10572–10577. https://doi.org/10.1073/pnas.1712381114

Fargione J, Tilman D (2005) Niche differences in phenology and rooting depth promote coexistence with a dominant C-4 bunchgrass. Oecologia 143:598–606. https://doi.org/10.1007/s00442-005-0010-y

Feddes RA, Hoff H, Bruen M, Dawson T, de Rosnay P, Dirmeyer O, Jackson RB, Kabat P, Kleidon A, Lilly A, Pitman AJ (2001) Modeling root water uptake in hydrological and climate models. Bull Am Meteorol Soc 82:2797–2809. https://doi.org/10.1175/1520-0477(2001)082<2797:mrwuih>2.3.co;2

Ferreira JN, Bustamante M, Garcia-Montiel DC, Caylor KK, Davidson EA (2007) Spatial variation in vegetation structure coupled to plant available water determined by two-dimensional soil resistivity profiling in a Brazilian savanna. Oecologia 153:417–430. https://doi.org/10.1007/s00442-007-0747-6

Fisher RA, Koven CD, Anderegg WRL, Christoffersen BO, Dietze MC, Farrior CE, Holm JA, Hurtt GC, Knox RG, Lawrence PJ, Lichstein JW, Longo M, Matheny AM, Medvigy D, Muller-Landau HC, Powell TL, Serbin SP, Sato H, Shuman JK, Smith B, Trugman AT, Viskari T, Verbeeck H, Weng ES, Xu CG, Xu XT, Zhang T, Moorcroft PR (2018) Vegetation demographics in earth system models: a review of progress and priorities. Glob Chang Biol 24:35–54. https://doi.org/10.1111/gcb.13910

Freschet GT, Roumet C (2017) Sampling roots to capture plant and soil functions. Funct Ecol 31:1506–1518. https://doi.org/10.1111/1365-2435.12883

Gile LH, Gibbens RP, Lenz JM (1998) Soil-induced variability in root systems of creosotebush (Larrea tridentata) and tarbush (Flourensia cernua). J Arid Environ 39:57–78. https://doi.org/10.1006/jare.1998.0377

Good SP, Noone D, Bowen G (2015) Hydrologic connectivity constrains partitioning of global terrestrial water fluxes. Science 349:175–177. https://doi.org/10.1126/science.aaa5931

Gray ST, Betancourt JL, Jackson ST, Eddy RG (2006) Role of multidecadal climate variability in a range extension of pinyon pine. Ecology 87:1124–1130. https://doi.org/10.1890/0012-9658(2006)87[1124:romcvi]2.0.co;2

Grossiord C, Sevanto S, Bonal D, Borrego I, Dawson TE, Ryan M, Wang WZ, McDowell NG (2019) Prolonged warming and drought modify belowground interactions for water among coexisting plants. Tree Physiol 39:55–63. https://doi.org/10.1093/treephys/tpy080

Hartle RT, Fernandez GCJ, Nowak RS (2006) Horizontal and vertical zones of influence for root systems of four Mojave Desert shrubs. J Arid Environ 64:586–603. https://doi.org/10.1016/j.jaridenv.2005.06.021

Jones HG (2007) Monitoring plant and soil water status: established and novel methods revisited and their relevance to studies of drought tolerance. J Exp Bot 58:119–130. https://doi.org/10.1093/jxb/erl118

Lajtha K, Barnes FJ (1991) Carbon gain and water-use in pinyon pine-juniper woodlands of northern new-mexico - field versus phytotron chamber measurements. Tree Physiol 9:59–67. https://doi.org/10.1093/treephys/9.1-2.59

Limousin JM, Bickford CP, Dickman LT, Pangle RE, Hudson PJ, Boutz AL, Gehres N, Osuna JL, Pockman WT, McDowell NG (2013) Regulation and acclimation of leaf gas exchange in a pinon-juniper woodland exposed to three different precipitation regimes. Plant Cell and Environment 36:1812–1825. https://doi.org/10.1111/pce.12089

Luo ZT, Niu JZ, Zhang L, Chen XW, Zhang W, Xie BY, Du J, Zhu ZJ, Wu SS, Li X (2019) Roots-enhanced preferential flows in deciduous and coniferous Forest soils revealed by dual-tracer experiments. J Environ Qual 48:136–146. https://doi.org/10.2134/jeq2018.03.0091

Manoli G, Huang CW, Bonetti S, Domec JC, Marani M, Katul G (2017) Competition for light and water in a coupled soil-plant system. Adv Water Resour 108:216–230. https://doi.org/10.1016/j.advwatres.2017.08.004

Martens SN, Breshears DD, Meyer CW, Barnes FJ (1997) Scales of above-ground and below-ground competition in a semi-arid woodland detected from spatial pattern. J Veg Sci 8:655–664. https://doi.org/10.2307/3237370

Meinzer FC, Woodruff DR, Marias DE, McCulloh KA, Sevanto S (2014) Dynamics of leaf water relations components in co-occurring iso- and anisohydric conifer species. Plant Cell and Environment 37:2577–2586. https://doi.org/10.1111/pce.12327

Mirfenderesgi G, Matheny AM, Bohrer G (2019) Hydrodynamic trait coordination and cost-benefit trade-offs throughout the isohydric-anisohydric continuum in trees. Ecohydrology 12. https://doi.org/10.1002/eco.2041

Morillas L, Pangle RE, Maurer GE, Pockman WT, McDowell N, Huang CW, Krofcheck DJ, Fox AM, Sinsabaugh RL, Rahn TA, Litvak ME (2017) Tree mortality decreases water availability and ecosystem resilience to drought in Pinon-Juniper woodlands in the southwestern US. Journal of Geophysical Research-Biogeosciences 122:3343–3361. https://doi.org/10.1002/2017jg004095

Neumann RB, Cardon ZG (2012) The magnitude of hydraulic redistribution by plant roots: a review and synthesis of empirical and modeling studies. New Phytol 194:337–352. https://doi.org/10.1111/j.1469-8137.2012.04088.x

Newman BD, Breshears DD, Gard MO (2010) Evapotranspiration partitioning in a semiarid woodland: Ecohydrologic heterogeneity and connectivity of vegetation patches. Vadose Zone J 9:561–572. https://doi.org/10.2136/vzj2009.0035

Peek MS, Leffler AJ, Hipps L, Ivans S, Ryel RJ, Caldwell MM (2006) Root turnover and relocation in the soil profile in response to seasonal soil water variation in a natural stand of Utah juniper (Juniperus osteosperma). Tree Physiol 26:1469–1476. https://doi.org/10.1093/treephys/26.11.1469

Pieper R (2008) Ecology of Piñon-Juniper vegetation in the southwest and Great Basin. In: Gottfried G, Shaw J, Ford P (eds) Ecology, management, and restoration of Piñon-Juniper and Ponderosa pine ecosystems: combined proceedings of the 2005 St George, Utah and 2006 Albuquerque, New Mexico workshops RMRS-P-51. U.S. Department of Agriculture, Forest Service, Rocky Mountain Research Station, Fort Collins, CP, USA

Pregitzer KS, DeForest JL, Burton AJ, Allen MF, Ruess RW, Hendrick RL (2002) Fine root architecture of nine north American trees. Ecol Monogr 72:293–309. https://doi.org/10.1890/0012-9615(2002)072[0293:fraonn]2.0.co;2

Redmond MD, Weisberg PJ, Cobb NS, Clifford MJ (2018) Woodland resilience to regional drought: dominant controls on tree regeneration following overstorey mortality. J Ecol 106:625–639. https://doi.org/10.1111/1365-2745.12880

Reid KD, Wilcox BP, Breshears DD, MacDonald L (1999) Runoff and erosion in a pinon-juniper woodland: influence of vegetation patches. Soil Sci Soc Am J 63:1869–1879. https://doi.org/10.2136/sssaj1999.6361869x

Renton M, Poot P (2014) Simulation of the evolution of root water foraging strategies in dry and shallow soils. Ann Bot 114:763–778. https://doi.org/10.1093/aob/mcu018

Ryel RJ, Leffler AJ, Ivans C, Peek MS, Caldwell MM (2010) Functional differences in water-use patterns of contrasting life forms in Great Basin Steppelands. Vadose Zone J 9:548–560. https://doi.org/10.2136/vzj2010.0022

Schenk HJ (2008a) The shallowest possible water extraction profile: a null model for global root distributions. Vadose Zone J 7:1119–1124. https://doi.org/10.2136/vzj2007.0119

Schenk HJ (2008b) Soil depth, plant rooting strategies and species' niches. New Phytol 178:223–225. https://doi.org/10.1111/j.1469-8137.2008.02427.x

Schenk HJ, Jackson RB (2002) The global biogeography of roots. Ecol Monogr 72:311–328. https://doi.org/10.1890/0012-9615(2002)072[0311:tgbor]2.0.co;2

Schenk HJ, Jackson RB (2005) Mapping the global distribution of deep roots in relation to climate and soil characteristics. Geoderma 126:129–140. https://doi.org/10.1016/j.geoderma.2004.11.018

Schlesinger WH, Jasechko S (2014) Transpiration in the global water cycle. Agric For Meteorol 189:115–117. https://doi.org/10.1016/j.agrformet.2014.01.011

Sperry JS, Wang YJ, Wolfe BT, Mackay DS, Anderegg WRL, McDowell NG, Pockman WT (2016) Pragmatic hydraulic theory predicts stomatal responses to climatic water deficits. New Phytol 212:577–589. https://doi.org/10.1111/nph.14059

Schwinning S, Hooten MM (2009) Mojave desert root systems. In: RH Webb, LF Fenstermaker, JS Heaton, DL Hughson, EV McDonald, DM Miller (eds) The Mojave Desert: Ecosystem Processes and Sustainability. University of Nevada Press, Reno, NV

Verhoef A, Egea G (2014) Modeling plant transpiration under limited soil water: comparison of different plant and soil hydraulic parameterizations and preliminary implications for their use in land surface models.

Agric For Meteorol 191:22–32. https://doi.org/10.1016/j.agrformet.2014.02.009

Walter H, Mueller-Dombois D (1971) Ecology of tropical and subtropical vegetation. Van Nostrand Reinhold Company, New York

Warren JM, Hanson PJ, Iversen CM, Kumar J, Walker AP, Wullschleger SD (2015) Root structural and functional dynamics in terrestrial biosphere models - evaluation and recommendations. New Phytol 205:59–78. https://doi.org/10.1111/nph.13034

Wilcox CS, Ferguson JW, Fernandez GCJ, Nowak RS (2004) Fine root growth dynamics of four Mojave Desert shrubs as related to soil moisture and microsite. J Arid Environ 56:129–148. https://doi.org/10.1016/s0140-1963(02)00324-5